Nuclear Magnetic Resonance Imaging of Syringomyelia

Andrew Yeates,[1,2] Michael Brant-Zawadzki,[1] David Norman,[1] Leon Kaufman,[1] Lawrence E. Crooks,[1] and Thomas H. Newton[1]

Five patients with syringomyelia were examined with a 3.5 kG nuclear magnetic resonance (NMR) imager. Syrinx cavities were visualized in all five cases, and image quality compared favorably with metrizamide computed tomography (CT). Axial images were optimal for identifying syrinx cavities, and sagittal views were useful in providing an overview of cord morphology and in examining the craniocervical junction. Inversion-recovery images were less valuable than the spin-echo sequences. By varying spin-echo imaging parameters, tissue relaxation times could be determined and the fluid nature of the syrinx cavities confirmed. This limited study suggests that NMR may challenge the current role of CT in the diagnostic workup of syringomyelia.

The rapid emergence of nuclear magnetic resonance (NMR) as a viable imaging modality has raised the question whether NMR has a unique role in specific disorders of the central nervous system. Potential advantages of NMR over computed tomography (CT) include more pronounced tissue contrast, direct multiplanar imaging, absence of artifacts associated with bone, potential for tissue characterization, and lack of ionizing radiation [1]. These properties appear well suited to imaging the spinal cord, particularly the absence of bone artifacts, which continue to degrade spinal CT image quality even in the most advanced CT units. As a preliminary assessment of the efficacy of NMR in spinal cord imaging, a small series of patients with syringomyelia was studied with both metrizamide CT and NMR.

Syringomyelia is a tubular cavitation of the spinal cord, most commonly affecting the cervical region but often extending to thoracic levels. Although it is distinct from hydromyelia, which is abnormal distention of the central canal, the two entities have similar gross appearances and may be difficult to distinguish even on pathologic examination [2]. In this discussion, therefore, the terms syringomyelia and hydromyelia will be used synonymously. In both entities, the abnormal fluid collections are generally of the same composition as cerebrospinal fluid (CSF).

Subjects and Methods

Five patients with known or suspected syringomyelia were studied with both metrizamide CT and NMR imaging. The series comprised three men and two women 48–60 years of age. The diagnosis of syringomyelia was surgically verified in all five patients. CT scans were obtained about 4 hr after subarachnoid injection of metrizamide. NMR imaging followed the CT scans by at least 24 hr. NMR images were routinely obtained in the axial plane. In three patients sagittal images were also generated. The cervical cord was examined in four patients and the thoracic cord in one patient. For comparison, NMR images of the cervical and thoracic cords, respectively, were obtained in normal volunteers and in patients without spinal disorders. Spin-echo sequences were used in all five syrinx patients; in three of these patients inversion-recovery images were also obtained. Because the inversion-recovery images were less satisfactory for identifying the syrinx cavities, this technique was abandoned in the remaining two patients.

The NMR imager at our institution is equipped with a 3.5 kG superconducting magnet. A 55 cm aperture was used for all studies. Spatial resolution was about 1.7 mm with a 128 × 128 matrix and a 7 mm slice thickness. Five adjacent sections were imaged simultaneously. Imaging time, related to the time interval between radiofrequency pulses, was 0.5–1.5 sec. This required a minimum image sequence time of 4.3 min for five sections and a maximum time of about 13 min for 15 sections.

Gray Scale

Intrinsic tissue properties affecting the intensity (I) of the received signal are the hydrogen density (H), spin-spin (T_2) and spin-lattice (T_1) relaxation times, and the flow of hydrogen atoms through the imaging field [f(V)]. The interrelation of these parameters is described by the equation $I = Hf(V)\ exp(-a/T_2)[1-exp(-b/T_1)]$ where a is the T_2 parameter (representing the time between application of the radiofrequency pulse and reception of the signal,) and b is the T_1 parameter (representing the time interval between application of successive radiofrequency pulses) [3].

From the above equation, the following statements can be derived: I increases when T_1 is shortened or T_2 is lengthened; when T_1 is very long compared with b, I will be low, independent of the value of T_2; when T_2 is short compared with a, I is also low, even if T_1 is short; lengthening of b increases I; lengthening of a decreases I and causes preferential enhancement of tissues with long values for T_2.

An important concept for our discussion is that the degree to which T_1 and T_2 relaxation times contribute to I depends on the values of b and a, respectively. Contrast between tissues with different relaxation times can, therefore, be made more or less pronounced by changing the imaging variables a and b.

This principle can be demonstrated with a spin-echo image taken through the lateral ventricles (fig. 1). When a equals 28 msec and b equals 1.5 sec, CSF is clearly seen as an area of low intensity compared with the brain. This is due to the long T_1 relaxation time of CSF. (*Note*: In general, fluids have a short T_1 and solids have a

[1] Department of Radiology, University of California, San Francisco, CA 94143.
[2] Present address: Department of Radiology, Box 3808, Duke University Medical Center, Durham, NC 27710. Address reprint requests to A. Yeates.

AJNR 4:234–237, May/June 1983 0195-6108/83/0403-0234 $00.00

long T_1. In biological systems, "pure" fluids such as CSF behave like solids in that they also have a relatively long T_1.) Also, note that gray matter produces a higher-intensity signal than white matter. When a is lengthened to 56 msec, CSF produces a stronger signal relative to brain parenchyma, reflecting the long T_2 relaxation time of CSF. (*Note*: In general, fluids have a long T_2, solids a short T_2.) This principle can also be demonstrated on direct sagittal images of the spinal cord and surrounding subarachnoid space (fig. 2).

CSF within a syrinx cavity would be expected to behave in the same manner as CSF with the brain. Therefore, a syrinx cavity successfully imaged using the spin-echo sequences described above would be seen as an area of low intensity within the spinal cord. A syrinx should not be confused with normal gray-white differentiation because gray matter emits a higher-intensity signal than the surrounding white matter, given the instrument parameters used in our material. In comparison, potential confusion can occur with inversion-recovery images, as both CSF and gray matter produce a lower-intensity signal than white matter [4].

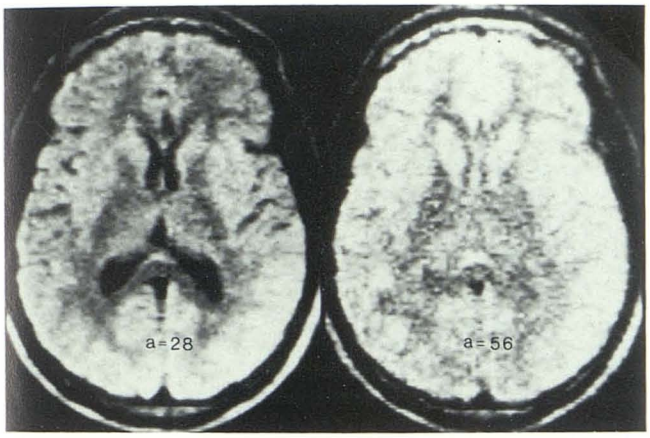

Fig. 1.—Axial spin-echo images at level of basal ganglia. When a = 28 msec (*left*), CSF produces very low-intensity signal. When a is lengthened to 56 msec (*right*), tissues with long T_2 relaxation times are selectively enhanced and CSF produces stronger signal relative to brain parenchyma. On both spin-echo sequences, gray matter produces higher-intensity signal than white matter. a = T_2 parameter.

Results

Normal Spinal Cord

In the spin-echo sequences used, the normal spinal cord in the cervical and thoracic region was visualized as an elliptical area of homogeneous signal intensity (fig. 3), clearly outlined by surrounding CSF. The signal intensity of the cord was slightly greater than that of the paravertebral muscles. The vertebral bodies showed a relatively high-intensity signal that varied according to the amount of fat within the bone marrow. At present, normal gray-white differentiation is not routinely identified with spin-echo images of the spinal cord, but is visualized by inversion-recovery techniques. Increased contrast resolution between gray and white matter on inversion-recovery images is obtained by using a lower signal-to-noise ratio than with spin-echo sequences.

Patients with Syringomyelia

Syrinx cavities were readily identified as areas of low intensity in the central portion of the spinal cord in all five patients with syringomyelia. The cavities were more clearly identified on spin-echo sequences than on inversion-recovery images. Not surprisingly, the axial plane was optimal for making the diagnosis of syringomyelia. Sagittal views were less satisfactory for syrinx visualization (fig. 4A). This is probably the result of volume-averaging the intensities of the syrinx cavity and adjacent cord parenchyma. Syrinx cavities are often irregular in configuration, and it is difficult to obtain a sagittal image that passes through the full thickness of the cavity over a long vertical distance. The sagittal projection was, however, useful in providing an overview of cord morphology and evaluating the craniocervical junction. A Chiari I malformation was present in one of the three patients examined with sagittal NMR projections (fig. 2). The appearance of the syrinx cavities varied from rather round, well circumscribed areas of low intensity (figs. 4B and 5) to horizontally oriented, less sharply demarcated areas of low intensity (fig. 6). The margins of the spinal cord were less sharp on the NMR

Fig. 2.—Direct sagittal images with spin-echo sequences. Cervical cord appears small with capacious surrounding subarachnoid space (*white arrows*) when a = 28 msec (*left*). Fourth ventricle is clearly visualized and cerebellar tonsils are caudally positioned (*black arrowhead*), consistent with Chiari I malformation. When a is lengthened to 56 msec (*right*), CSF around cord and in fourth ventricle becomes more isodense with parenchyma, giving false impression of cord enlargement. a = T_2 parameter.

Fig. 3.—Axial spin-echo image. Normal midcervical spinal cord. When a = 28 msec and b = 1.0 sec, cord (*arrowhead*) produces homogeneous signal and is clearly outlined by CSF. a = T_2, b = T_1 parameter.

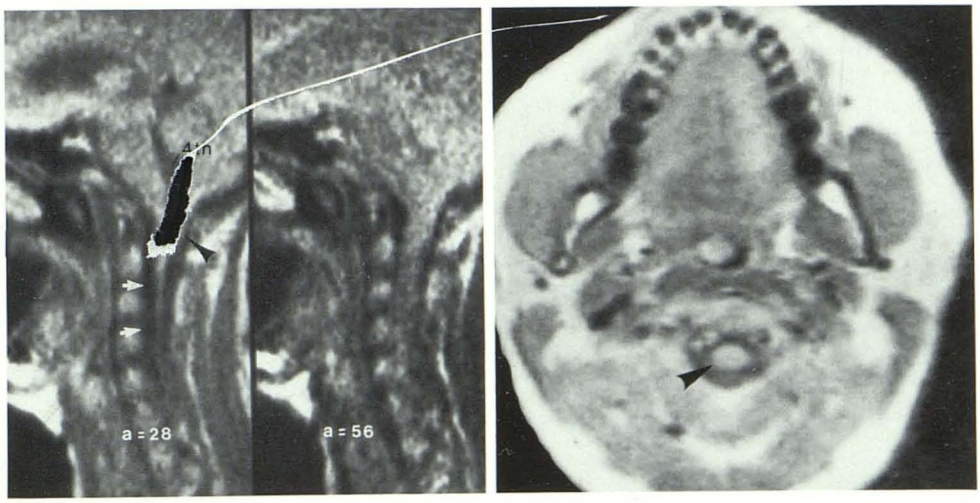

2 3

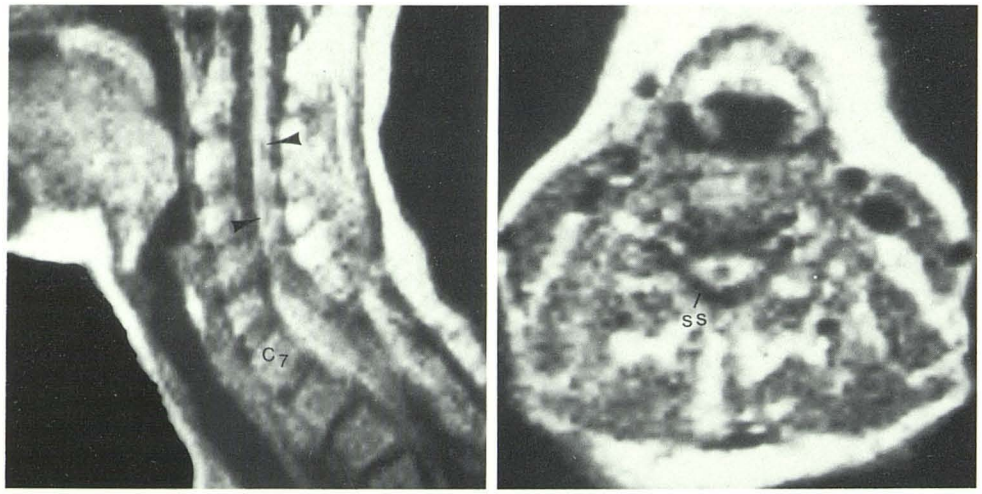

Fig. 4.—Syringomyelia. **A**, Direct sagittal spin-echo image. Fusiform enlargement of cord at cervicothoracic junction. Syrinx cavity can be identified as thin, vertically oriented area of low intensity (*arrowheads*), but is more clearly shown in *B*, axial spin-echo image from same patient (a = 28 msec, b = 1.5 sec), where syrinx appears as rounded area of low intensity, well circumscribed from adjacent cord. Surrounding subarachnoid space (ss) is also clearly visualized. a = T_2, b = T_1, parameter.

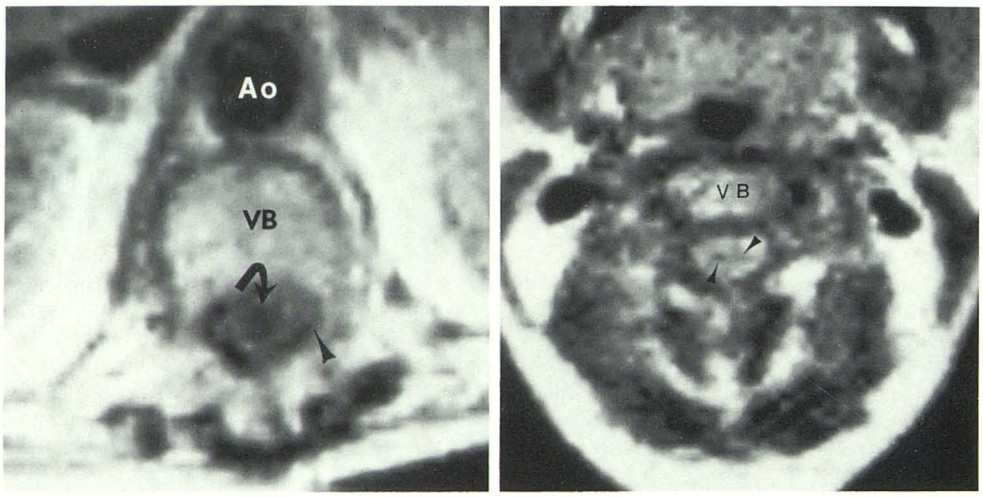

Fig. 5.—Axial spin-echo image. Lower thoracic syrinx (*curved arrow*) appears as round area of low intensity in enlarged thoracic cord. Margins of cord are somewhat irregular and poorly defined due to arachnoidal adhesions and scarring (*arrowhead*), which had previously appeared on myelography and metrizamide CT. VB = vertebral body, Ao = aorta.

Fig. 6.—Syringomyelia. Axial spin-echo image. Metrizamide CT showed enlarged cervical cord without opacification of syrinx, suggesting intramedullary tumor. NMR image also demonstrates enlarged cervical cord, while syrinx cavity (*arrowheads*) is seen as horizontally-oriented area of low intensity, rather poorly circumscribed from adjacent cord parenchyma. VB = vertebral body.

images than in metrizamide CT studies, although the ability to assess cord size and overall morphology was comparable in the two modalities.

In four of the five patients, the syrinx cavities were visualized on delayed metrizamide CT. The CT scan in the fifth patient showed an enlarged cervical cord, but the syrinx cavity failed to opacify with metrizamide. It is difficult to make a definitive statement about relative contrast between syrinx cavities and surrounding cord on NMR versus metrizamide CT, as the density of the syrinx in the latter is a function of the amount of metrizamide used and the degree to which the metrizamide diffuses into the cavity.

On the spin-echo images, maximum contrast between syrinx cavity and spinal cord was obtained by using the imaging variable of a = 28 msec and b = 1.5 sec. Lengthening a to 56 msec made the cavity appear more isodense as compared with the surrounding cord (fig. 7), confirming that the area of low density did, in fact, have a long T_2 relaxation time compatible with fluid.

Discussion

The radiographic evaluation of syringomyelia has evolved from myelography, which was aimed at defining spinal cord size and morphology, to CT, with the intent of directly visualizing the syrinx cavity. Despite roughly a 15–20 Hounsfield-unit difference between neural tissue and CSF, opacification of the syrinx with intrathecal injection of metrizamide is generally required for reliable CT visualization [5]. This is due primarily to image degradation caused by surrounding bone. An estimated 80%–90% of syrinx cavities will be identified using high-resolution metrizamide CT [6–8].

Our early experience with NMR as a method of investigating syringomyelia is encouraging. Syrinx cavities were readily identified as areas of low intensity relative to the surrounding cord in all five patients diagnosed with the disease. Moreover, the fluid nature of the cavities could be confirmed by changing the imaging parameters allowing characterization of tissue T_1 and T_2 relaxation times. Sag-

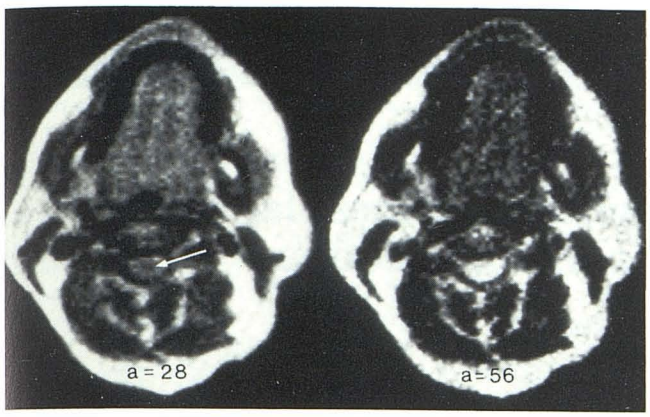

Fig. 7.—Syringomyelia. Axial spin-echo images. When a = 28 msec, syrinx (*arrow*) is seen as central area of low intensity (*left*). When a = 56 msec (*right*), cavity becomes isodense with surrounding spinal cord parenchyma, consistent with fluid (long T_2 relaxation time). a = T_2 parameter.

ittal views were easily obtained and were useful in obtaining an overview of cord morphology. They were particularly helpful in examining the craniocervical junction, which is usually an area of interest in patients with syringomyelia because of the high incidence of associated Chiari I malformations [5], but were less reliable than axial views for identifying the syrinx cavity. Spin-echo sequences were superior to inversion-recovery images in the evaluation of syringomyelia. Inversion-recovery images produce a lower signal-to-noise ratio and are potentially confusing because normal gray- and white-matter intensity differences may be mistaken for a syrinx cavity. This potential problem can be avoided by selecting spin-echo imaging parameters in which gray matter produces a higher-intensity signal than surrounding white matter.

Our small series of patients does not represent a rigorous comparison of the relative merits of NMR and metrizamide CT in the evaluation of syringomyelia. The CT scans were performed before the NMR examinations, had already provided the diagnosis of syringomyelia in four of the five patients, and were used to help determine the areas to be examined by NMR.

An important question is whether NMR will be able to distinguish cystic tumors from syrinx cavities. Impurities within any fluid collection should shorten T_1 relaxation time. Intramedullary fluid containing blood or markedly elevated protein would therefore not be expected to produce the low-intensity signal seen in a typical syrinx. Clearly, further experience in imaging both syringomyelia and spinal cord tumors is required to determine the usefulness of NMR in this regard.

NMR appears to offer an alternative to metrizamide CT in the study of syringomyelia, although additional experience is needed to accurately weigh the relative merits of NMR against what has proven to be a very sensitive and reliable imaging technique. The potentials for tissue characterization and direct multiplanar imaging, as well as the ability to demonstrate syrinx cavities without the use of intrathecal contrast material, suggest that the role of NMR will be a prominent one.

REFERENCES

1. Crooks L, Hoenninger J, Arakawa M, et al. Tomography of hydrogen with nuclear magnetic resonance. *Radiology* **1980;** 136:701–706
2. Blackwood W, Corsellis JAN, eds. Syringomyelia and syringobulbia. In: *Greenfield's neuropathology*. London: Arnold, **1977:**668–674
3. Crooks LE, Mills CM, Davis PL, et al. Visualization of cerebral and vascular abnormalities by NMR imaging. The effects of imaging parameters on contrast. *Radiology* **1982;**144:843–852
4. Young IR, Bailes DR, Burl M, et al. Initial clinical evaluation of a whole body nuclear magnetic resonance (NMR) tomograph. *J Comput Assist Tomogr* **1982;**6:1–18
5. Cahan LD, Bentson JR. Considerations in the diagnosis and treatment of syringomyelia and the Chiari malformation. *J Neurosurg* **1982;**57:24–31
6. Aubin ML, Vignaud J, Jardin C, Bar D. Computed tomography in 75 clinical cases of syringomyelia. *AJNR* **1981;**2:199–204
7. Bonafe A, Manelfe C, Espagno J, Guiraud B, Rascol A. Evaluation of syringomyelia with metrizamide computed tomographic myelography. *J Comput Assist Tomogr* **1980;**4:797–802
8. Resjo IM, Harwood-Nash DC, Fitz CR, Chuang S. Computed tomographic metrizamide myelography in syringomydromyelia. *Radiology* **1979;**131:405–407